

BRIEF REPORT

Providing octane degradation capability to *Pseudomonas putida* KT2440 through the horizontal acquisition of oct genes located on an integrative and conjugative element

Estrella Duque¹  | Zulema Udaondo²  | Lázaro Molina¹  |
Jesús de la Torre¹  | Patricia Godoy¹  | Juan L. Ramos¹ 

¹Department of Environmental Protection, Estación Experimental del Zaidín, CSIC, Granada, Spain

²Department of Biomedical Informatics, University of Arkansas for Medical Science, Little Rock, Arkansas, USA

Correspondence

Juan L. Ramos, Department of Environmental Protection, Estación Experimental del Zaidín, CSIC, c/Profesor Albareda 1, 1808 Granada, Spain.

Email: juanluis.ramos@eez.csic.es

Funding information

Ministerio de Ciencia y Tecnología, Grant/Award Number: RT12018-094370-B-I00

Abstract

The extensive use of petrochemicals has produced serious environmental pollution problems; fortunately, bioremediation is considered an efficient way to fight against pollution. In line with Synthetic Biology is that robust microbial chassis with an expanded ability to remove environmental pollutants are desirable. *Pseudomonas putida* KT2440 is a robust lab microbe that has preserved the ability to survive in the environment and is the natural host for the self-transmissible TOL plasmid, which allows metabolism of toluene and xylenes to central metabolism. We show that the *P. putida* KT2440 (pWW0) acquired the ability to use octane as the sole C-source after acquisition of an almost 62-kb ICE from a microbial community that harbours an incomplete set of octane metabolism genes. The ICE bears genes for an alkane monooxygenase, a PQQ-dependent alcohol dehydrogenase and aldehyde dehydrogenase but lacks the electron donor enzymes required for the monooxygenase to operate. Host rubredoxin and rubredoxin reductase allow metabolism of octane to octanol. Proteomic assays and mutants unable to grow on octane or octanoic acid revealed that metabolism of octane is mediated by redundant host and ICE enzymes. Octane is oxidized to octanol, octanal and octanoic acid, the latter is subsequently acylated and oxidized to yield acetyl-CoA that is assimilated via the glyoxylate shunt; in fact, a knockout mutant in the *aceA* gene, encoding isocitrate lyase was unable to grow on octane or octanoic acid.

INTRODUCTION

Over the last century, the chemical industry has been based on the exploitation of petrochemicals as fuels for combustion and as raw materials for the synthesis of a wide range of compounds. Many of these chemicals reach the environment, and while some are degraded others remain in soils or water either because of their recalcitrance or their rate of deposit is still far superior to that of removal (Danso et al., 2019; Mori & Kanaly, 2021; Nagata et al., 2019). Pollution related to

petrochemical use has led to global warming and the search is now on to replace polluting chemicals with new green alternatives (Calero & Nickel, 2019; García-Franco et al., 2021; Godoy et al., 2021; Ramos & Duque, 2019); although the new (bio)chemistry for production of chemicals is still developing (Brooks & Alper, 2021; Liu et al., 2020; Reed & Alper, 2018).

Bioremediation is an efficient way to fight against pollution and to warrant environmental performance, biodegradation platforms that are able to remove multiple pollutants are of interest. In the selection of such

This is an open access article under the terms of the [Creative Commons Attribution-NonCommercial-NoDerivs](https://creativecommons.org/licenses/by-nc-nd/4.0/) License, which permits use and distribution in any medium, provided the original work is properly cited, the use is non-commercial and no modifications or adaptations are made.

© 2022 The Authors. *Environmental Microbiology Reports* published by Society for Applied Microbiology and John Wiley & Sons Ltd.

microorganisms, it must be noted that some pollutants are intrinsically toxic (Beites & Mendes, 2015; Ramos et al., 2015; Whyte et al., 1997). Hence, the selection of biodegradation platforms should be based not only on the basic metabolic potential of the microorganisms but also on their endurance and stress responses. Current legislation limits the use of recombinant microbes in the environment and for this reason microbes that have naturally acquired catabolic genes for removal of pollutants should be considered as a preferential way to build new pathways to expand their metabolic potential (Ramos & Timmis, 1987; Reineke & Knackmuss, 1988).

The soil bacterium *Pseudomonas putida* survives well in soils and is highly tolerant to hydrocarbons and xenobiotic compounds. Thus, it has the potential to serve as a robust platform for the degradation of chemicals. Pangenome analysis of the species has revealed a series of core genes that provide it with a versatile central metabolism, and which enable it to metabolize natural and xenobiotic compounds. In addition, strains of this species are endowed with a series of efflux pumps that extrude toxic chemicals from the cytoplasm, the periplasm and the outer membrane to the surrounding medium to provide a defensive mechanism against toxic chemicals (reviewed by Udaondo et al., 2012; Ramos et al., 2015; Udaondo et al., 2016). Furthermore, their metabolic potential allows bacteria of this species to adapt to rapidly changing conditions (e.g. oxidative stress, temperature challenges and sudden osmotic perturbations) (Cuenca et al., 2016a; Cuenca et al., 2016b; Matilla et al., 2007; Molina-Santiago et al., 2014; Nikel & de Lorenzo, 2013; Nikel & de Lorenzo, 2014; Nogales et al., 2020). As such, the core functions define the *P. putida* species as a robust chassis for environmental survival and operation (Belda et al., 2016; Molina et al., 2000; Nogales et al., 2020; Udaondo et al., 2016). Analysis of *P. putida* accessory genes also revealed a number of catabolic properties shared by two or more strains but not all, for example, chromosomally encoded pathways for degradation of aromatic hydrocarbons—the *tod* pathway (Zylstra & Gibson, 1989) or pathways linked to self-transmissible plasmids—the TOL plasmid for degradation of toluene via the toluene monooxygenase pathway (Worsey & Williams, 1975).

Pseudomonas putida KT2440 strain is a derivative of *P. putida* mt-2, which was isolated as a degrader of 3-methylbenzoic acid from a soil sample in Japan in 1960 (Nakazawa, 2002). This metabolic property was linked to the presence of the catabolic self-transmissible TOL plasmid pWW0, which encodes a set of enzymes that enable *P. putida* to grow on several aromatic hydrocarbons such as toluene, *m*-xylene and *p*-xylene (Bagdasarian et al., 1981; Worsey & Williams, 1975). The strain has also been subjected to mutagenesis and subsequent selection to isolate clones able to degrade recalcitrant chemicals such as

p-ethylbenzoate (Ramos et al., 1987). *Pseudomonas putida* KT2440 strain is a well-characterized member of this species and has become a model laboratory microbe for bioremediation. It has also retained its ability to survive and thrive in edaphic and aquatic environments despite a long history in the laboratory (Molina et al., 2000). The strain was included as part of a bacterial consortium used to remove petroleum-based hydrocarbons from soils (Pizarro-Tobias et al., 2015). In this niche it is resilient; field tests revealed that the strain could survive for months in the roots of plants (Molina et al., 2000; Niqui-Arroyo et al., 2013; Ronchel & Ramos, 2001). *In silico* analysis of the 6,181,873 bp long genome sequence of *P. putida* KT2440 (Belda et al., 2016; Nelson et al., 2002) revealed the lack of any virulence factor in the genome, which was the basis of the early designation of the strain as a generally safe host for recombinant DNA constructs and use in the environment (Kampers et al., 2019; Nikel & de Lorenzo, 2018; Poblete-Castro et al., 2013; Poblete-Castro et al., 2020; Timmis, 2002). The genome of KT2440 encodes a broad array of enzymes that can remove oxygen-free radicals, i.e. superoxide dismutase, peroxidases and other enzymes capable of dealing with oxidative agents.

In a previous study, Niqui-Arroyo et al. (2013) described a consortium of microorganisms that grew well with a wide range of linear (i.e. octane, decane, dodecane) and branched hydrocarbons present in wastewaters generated by cleaning airport runways. Analysis of the 16S rRNA amplicons of this consortium revealed a wide range of microbes belonging to genus *Acinetobacter*, *Brevibacterium*, *Sphingobium*, *Cupriavidus*, *Yersinia*, *Alteromonas* and others. Unfortunately, certain limitations prevent the direct use of the consortium as a bioremediation agent. Namely, some of the microbes have potentially pathogenic characters and certain bacteria could not be recovered and cultured on solid agar plates. To overcome these limitations, we hypothesized that it would be possible to rescue the catabolic potential of the bacteria in hydrocarbon-enriched samples (i.e. the ability to degrade linear hydrocarbons) by incorporating the corresponding genes via natural gene transfer into the KT2440 (pWW0) chassis (Nogales et al., 2020). This was carried out to enhance the ability of KT2440 to catabolize and degrade pollutants.

RESULTS AND DISCUSSION

Achieving octane degradation in *Pseudomonas putida* KT2440 (pWW0)

Because some of the octane-degrading microorganisms in the consortium did not grow on solid medium (Niqui-Arroyo et al., 2013) we chose to carry out liquid culture matings to transfer genes to KT2440 and enable

the strain to grow on linear hydrocarbons. We set up liquid mating by mixing 1 ml of KT2440 (pWW0) grown with toluene as the sole C-source and 1 ml of the consortium supplied by Bio-Ilberis R&D. The mixed cultures were kept at 30°C with soft agitation. To counter select the KT2440 (pWW0) capable of degrading octane, we spread 0.1 ml of the mating culture on M9 minimal medium plates with octane as the sole C-source and 30 µg ml⁻¹ of rifampicin—an antibiotic that KT2440 is resistant to but that none of the consortium bacteria is resistant to. The rate of appearance of Rif^R Oct⁺ colonies on these plates was 1 out 10⁹ per recipient cell.

To test if the colonies on the plates were derived from KT2440 (pWW0), we performed a series of quick metabolic tests which consisted of checking that the cells used three carbon sources: (i) toluene, which is assimilated through the upper and *meta* cleavage pathway of the TOL plasmid present in the original recipient cells (Worsey & Williams, 1975); (ii) citrate, a tricarboxylic acid that *P. putida* is able to transport into the cytoplasm and is used as a sole carbon and energy source (Herrero et al., 1990); and (iii) the newly acquired property of degrading octane. In all cases all strains were positive. To further assure that KT2440 was the host, we used the 27F (5'-AGAGTTTGATCTGGCTCAG-3') and 1492R (5'-GGCTCGAGCGGCCGCCCCGGG-3') primers and amplified the 16S rRNA gene. The sequences we obtained matched >99% to those of *P. putida* KT2440, which led us to believe that KT2440 (pWW0) had acquired the genes involved in the degradation of octane. Because matings were kept for 48 h, we cannot discard siblings and for this reason a random colony, which we named EM2-4, was chosen for further characterization. The EM2-4 strain was able to grow exponentially on octane with duplication times of 105–120 min and yields of about 0.36–0.4 CDW g⁻¹ octane. Surprisingly the strain did not use any other medium-chain or branched hydrocarbons.

It is known that *P. putida* cells exposed to hydrocarbons fortify their membranes by isomerization of both C16 and C18 *cis* fatty acids to the *trans* forms. In agreement with this observation is that the *cis:trans* ratio of EM2-4 changed from about 5.9–7.8 in glucose grown cells to 1.04–1.14 in cells growing on octane (Table S1). Similar results have been reported before for several *Pseudomonas* strains (Chen et al., 1995). As such, the acquisition of the ability to grow on octane at a high rate does not preclude one of the toxic chemical stress responses of the *P. putida* KT2440 strain.

Sequence analysis of the genome of *P. putida* EM2-4

We sequenced the genome of strain EM2-4 using Illumina and a genome coverage of 200×. The 6.2 Mb genome was comprised of 78 contigs with sizes

ranging between 43,286 and 549,539 bp. We found a contig of 66,272 bp that contained a 61,974 bp insert with flanking chromosomal DNA, which allowed us to identify that the set of genes was on the chromosome and not on the TOL plasmid. In fact, the genetic element gained was located between PP_4491 (*phhB*, which encodes a pterin-4- α -carbinolamine dehydratase involved in the folate biosynthetic pathway) and PP_4492 (*yhhS*, which encodes a carbohydrate efflux transporter) (Figure 1). Sequence analysis supported that the acquired DNA with a G + C of 64.86% and encoding 58 ORFs corresponded to an integrative conjugative element (ICE) confirmed by using ICEberg v2.0 database (<https://db-mm1.sjtu.edu.cn/CEfinder.html>) (Johnson & Grossman, 2015; Liu et al., 2019). The online tool from ICEberg database, ICEfinder detects recombination and conjugation modules in the query DNA sequence using Hidden Markov Models and then looks for the *oriT* region, then it performs a pattern-based colocalization of gene groups in the element (Li et al., 2018). Further analysis comparing the ICE acquired by *P. putida* against other elements in the ICEberg dataset revealed that several ICE modules of the ICE genes are present on chromosomes or plasmids of multiple microorganisms from different taxa. It appears that the ICE present in KT2440 gained successive sets of genes that most likely originated from *Burkholderia*, *Delftia*, *Aeromonas*, *Ralstonia*, *Shewanella*, *Paraburkholderia* and others (see Table 1). The set of ORFs present on the ICE was distributed into three defined regions (Table 1; Figure 1). The first one is flanked by an integrase (ORF1 of the ICE) and a series of IS5, IS6, IS21 and IS478 sequences (ORFs 33–39 in Table 1). This region was populated by genes that encoded proteins of unknown function, and an efflux pump (ORF23–25). Downstream, a second region contains seven genes putatively involved in the degradation of alkanes, namely: ORF41, which encodes an alkane 1-monooxygenase that could oxidize octane into octanol; ORF42, a quinone-dependent alkan-1-ol dehydrogenase that transforms octanol to the corresponding aldehyde; ORF44, an aldehyde dehydrogenase that transforms octanol to octanoic acid; and ORF43, a putative acyl-CoA ligase that permits the entry to the acylated fatty acid to the β -oxidation cycle (Table 1), and two transcriptional regulators that belong to the LysR and AraC families. In addition, we found 13 proteins (from ORF46 to ORF58) which encode a series of transfer functions of the P-type conjugative system (i.e. TrbCBJKLFGI).

Alkane monooxygenases of *Pseudomonas* GPO1 that hydroxylate medium-chain hydrocarbons usually comprise three components: (i) the AlkB monooxygenase (51% identity with ORF41 in the ICE acquired by EM2-4), (ii) a soluble NADH-rubredoxin reductase and (iii) the soluble transfer protein rubredoxin (Alonso & Roujeinikova, 2012; Chen et al.,

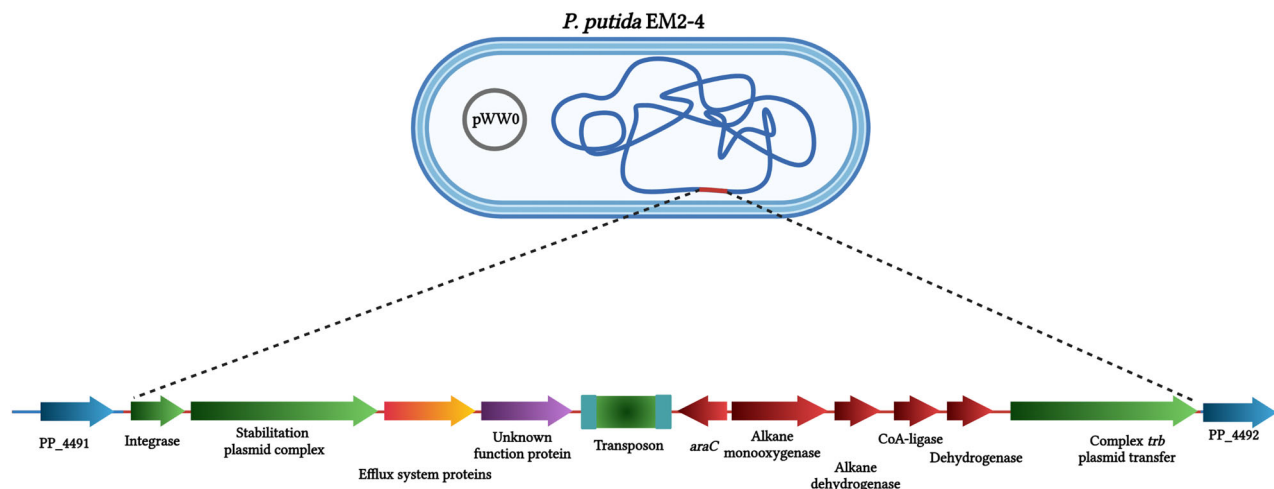


FIGURE 1 Schematic representation of the ICE acquired for octane degradation by M2-4. Arrows indicate direction of transcription. The ORFs are shown: in green are gene clusters related to DNA transfer and stabilization; in orange an efflux pump of the RND family; in red genes related to octane degradation

1995). The *alk* cluster in EM2-4 is atypical in the sense that genes encoding electron donors of the monooxygenase, such as the rubredoxin oxidoreductase or rubredoxin, were not present. Therefore, we assumed that host proteins would participate in ALK reaction electron transfers (Li et al., 2019; Rojo, 2009).

More concretely, the genome of *P. putida* KT2440 contains a gene (PP_5315 or *rubA*) that encodes a rubredoxin-I and two genes (*alkT* or PP_5314 and PP_5371) encoding two rubredoxin-NAD(+) reductases; enzymes responsible of the reduction of oxidized rubredoxins. Therefore, the acquisition of the octane degradation capability by *P. putida* KT2440 appears to be the result of a new pathway made of acquired environmental genes and host genes, which work coordinately.

We tested if the ICE element was stable and if it can be transferred to other strains. We grew EM2-4 cells for 100 generations in LB and then cells were spread on M9 with toluene as sole C-source, M9 with octane as the sole C-source, or M9 with citrate as the sole C-source. All of the cells were able to grow in each condition, suggesting stable inheritance of the ICE element.

To test if the ICE can be transferred horizontally to other *Pseudomonas* strains, we mated EM2-4 with *P. putida* PSC303 and PSC2078, two Km^R derivatives of KT2440 marked with a mini-Tn5, that grow on citrate as a C-source but not on octane (del Castillo et al., 2008). Donor and recipient cells were harvested in the mid logarithmic phase or in the late stationary phase and the mattings were done on solid LB medium plates, M9 minimal medium plates with glucose as a C-source and in liquid M9 medium for up to 24 h. No Km^R Oct⁺ clones were recovered indicating that the rate of transfer of the ICE element under these conditions is below 10⁻¹⁰ per recipient.

Proteomic analysis reveals how octane is channelled to central metabolism in this strain

Given that EM2-4 grew exponentially with octane and that the ICE was genetically stable, we endeavoured to further characterize the phenotype. We carried out proteomic analysis to define the route through which the cells metabolize the linear hydrocarbon.

For this, three replicates were performed in two different growth conditions: M9 with glucose (control), and M9 with octane (0.5%, vol./vol.) as sole carbon source (octane metabolism). Doubling times in the exponential phase with glucose (97 ± 3 min) and octane (110 ± 5 min) were similar, and cells were harvested by centrifugation at the mid-log phase (14,000g 5 min) when cultures had reached a turbidity of about 0.8 at OD₆₆₀. Cell pellets were frozen at -80°C until used and lysed as previously described (Molina et al., 2019). The proteins were digested with trypsin after reduction of disulfur bridges with 100 mM Tris-carboxyethyl-phosphine, then alkylated with 200 mM chloroacetamide (see Supplementary Experimental procedures) and finally TMT-6plex labelled (Altelaar et al., 2013). Then, peptides were identified by high-throughput-tandem mass spectrometry and quantified as described in the Supplementary Experimental procedures. We compared the control condition (glucose) with cells grown in octane as sole carbon source in terms of protein enrichment using the T-fold method of PROTEOBIOTICS, as recommended by the Proteomic Facility of CNB. A total of 2677 different quantification peptide groups were confidently assigned (Table S2; data are hosted on figshare and available via <https://figshare.com/s/d5bc13bcb41bdaf951fc> and DOI: 10.6084/m9.figshare.17061629). Their relative quantities were

TABLE 1 ORFs present in the ICE and identification of the genetic clusters

ORF	Amino acids	Function	BlastN best hit NCBI nr/nt bacteria database				
			Organism	ORF	Query cover	Percent intent	E-value
0	119	Pterin-4-alpha-carbinolamine dehydratase	<i>Pseudomonas putida</i>	PP_491			
1	401	Integrase	<i>Burkholderia cenocepacia</i>	A3203_15290	99	96.33	0.0
2	355	Nuclease domain-containing protein	<i>Delftia lacustris</i>	I6G47_25115	100	93.02	0.0
3	170	DNA repair protein RadC	<i>Pseudomonas aeruginosa</i>	EIP87_28665	100	95.69	0.0
4	117	Mlr6156 protein	<i>Pseudomonas putida</i>	E6B08_23585	100	97.72	4.00E-169
5	93	Hypothetical protein	<i>Pseudomonas putida</i>	E6B08_23580	100	95.34	6.00E-121
6	84	Hypothetical protein	<i>Aeromonas</i> sp.	C2U47_04775	100	98.81	4.00E-122
7	277	UPF0380 proteins YafZ and homologues	<i>Burkholderia cenocepacia</i>	A3203_15330	100	96.99	0.0
8	688	Putative plasmid stabilization protein, ParB	<i>Aeromonas caviae</i>	WP3S18E02_07940	100	92.89	0.0
9	105	y4eB gene homologue	<i>Pseudomonas aeruginosa</i>	K0E62_28125	100	98.1	2.00E + 152
10	111	Transcriptional regulator, Xre family	<i>Pseudomonas aeruginosa</i>	MCN99_21695	98	96.34	1.00E-149
11	117	Putative lipoprotein	<i>Burkholderia cenocepacia</i>	A3203_15355	100	96.58	0.0
12	60	Hypothetical protein	<i>Burkholderia cenocepacia</i>	CP015036 (3492922... 3493101)	100	99.44	4.00E-71
13	257	Hypothetical protein	<i>Burkholderia cenocepacia</i>	A3203_15360	100	94.81	0.0
14	95	Helix–turn–helix domain-containing protein	<i>Delftia lacustris</i>	I6G47_25210	100	96.14	1.00E-127
15	286	Plasmid replication initiator protein	<i>Ralstonia solanacearum</i>	RSc2606	100	95.45	0.0
16	73	Hypothetical protein	<i>Enterobacter</i> sp.	CU081_17605	100	97.65	3.00E-119
17	213	ParA-like protein	<i>Pseudomonas aeruginosa</i>	CWI20_06980	100	94.21	0.0
18	91	ParB-like protein	<i>Thioalkalivibrio sulfidiphilus</i>	Tgr7_1880	100	93.41	3.00E-109
19	186	Hypothetical protein	<i>Pseudomonas aeruginosa</i>	EIP87_28580	100	94.99	0.0
20	200	S26 family signal peptidase	<i>Sphingomonas</i> sp.	EIK56_27525	93	92.50	0.0
21	43	VirD2 components relaxase	<i>Variovorax paradoxus</i>	CP091716 (1641334... 1641462)	100	90.77	1.00E-39
22	665	VirD2 components relaxase	<i>Burkholderia cenocepacia</i>	A3203_15395	100	97.46	0.0
23	296	Efflux RND transporter periplasmic adaptor subunit, mdtA	<i>Shewanella chilikensis</i>	GII14_05840	100	95.5	0.0
24	1108	Efflux RND transporter permease subunit, mdtB	<i>Thauera</i> sp.	Tmz1t_2073	100	93.8	0.0
25	495	Efflux transporter outer membrane subunit, outer membrane factor (OMF) lipoprotein	<i>Thauera</i> sp.	Tmz1t_2072	100	93.36	0.0

(Continues)

TABLE 1 (Continued)

ORF	Amino acids	Function	BlastN best hit NCBI nr/nt bacteria database				
			Organism	ORF	Query cover	Percent intent	E-value
26	583	Ubiquinone biosynthesis protein UbiB	<i>Diaphorobacter</i> sp.	I3K84_20315	93	93.8	0.0
27	325	Patatin-like phospholipase family protein	<i>Variovorax paradoxus</i>	L3V85_07690	100	99.79	0.00E + 00
28	254	Octaprenyl diphosphate synthase	<i>Hydrogenophaga pseudoflava</i>	HPF_12290	100	96.33	0.0
29	898	Processive diacylglycerol beta-glucosyltransferase	<i>Hydrogenophaga pseudoflava</i>	HPF_12295	100	96.51	0.0
30	234	CerR family C-terminal domain-containing protein	<i>Hydrogenophaga pseudoflava</i>	HPF_12300	100	99.72	0.0
31	203	Hypothetical protein	<i>Hydrogenophaga pseudoflava</i>	HPF_12305	100	99.51	0.0
32	236	Hypothetical protein	<i>Hydrogenophaga pseudoflava</i>	HPF_12310	100	98.59	0.0
33	113	Transposase	<i>Variovorax paradoxus</i>	L3V85_07650	100	100.00	8.00E-176
34	107	IS66 family insertion sequence element accessory protein TnpB	<i>Variovorax paradoxus</i>	L3V85_07645	100	100.00	3.00E-149
35	511	IS66 family transposase	<i>Variovorax paradoxus</i>	L3V85_07640	100	100.00	0.0
36	418	IS5 family transposase	<i>Acidovorax</i> sp.	BSY15_3119	100	90.91	0.0
37	515	IS21 family transposase	<i>Acidovorax</i> sp.	Ajs_3594	100	93.72	0.0
38	246	IS21-like element helper ATPase IstB	<i>Comamonas thiooxydans</i>	LCH15_25240	100	94.04	0.0
39	94	IS1478 transposase	<i>Acidovorax</i> sp.	BSY15_166	91	92.66	9.00E-100
40	371	AraC family transcriptional regulator	<i>Variovorax paradoxus</i>	L3V85_07635	100	99.91	0.0
41	754	Alkane-1 monooxygenase	<i>Variovorax paradoxus</i>	L3V85_07630	100	99.96	0.0
42	559	Alkan-1-ol dehydrogenase, PQQ-dependent	<i>Variovorax paradoxus</i>	L3V85_07625	100	100.00	0.0
43	542	3-Methylmercaptopropionyl-CoA ligase	<i>Variovorax paradoxus</i>	L3V85_07620	100	99.94	0.0
44	580	Aldehyde dehydrogenase	<i>Variovorax paradoxus</i>	L3V85_07615	100	99.94	0.0
45	315	Transcriptional regulator, LysR family	<i>Variovorax paradoxus</i>	L3V85_07610	100	100.00	0.0
46	93	Entry exclusion lipoprotein TrbK	<i>Variovorax paradoxus</i>	L3V85_07605	100	100.00	1.00E-142
47	678	Conjugal transfer protein TraG	<i>Variovorax paradoxus</i>	L3V85_07600	100	100.00	0.0
48	159	CopG family transcriptional regulator	<i>Variovorax paradoxus</i>	L3V85_07595	100	100.00	0.0
49	355	P-type conjugative transfer ATPase TrbB	<i>Variovorax paradoxus</i>	L3V85_07590	100	100.00	0.0
50	130	Conjugative transfer protein TrbC, TrbC/VirB2	<i>Variovorax paradoxus</i>	L3V85_07585	100	100.00	0.00E + 00
51	91	Family type IV secretion system protein, TrbB/VirB3	<i>Variovorax paradoxus</i>	L3V85_07580	100	100.00	0.00E + 00
52	825	Conjugative transfer protein TrbE	<i>Pseudomonas aeruginosa</i>	PERCYII40_2689	100	91.53	0.0
53	252	Conjugative transfer protein TrbJ	<i>Comamonas</i> sp.	FOZ74_04005	100	93.83	0.0

(Continues)

TABLE 1 (Continued)

ORF	Amino acids	Function	BlastN best hit NCBI nr/nt bacteria database				
			Organism	ORF	Query cover	Percent intent	E-value
54	95	Conjugative transfer protein TrbK	<i>Pseudomonas aeruginosa</i>	FOY97_18900	100	96.84	6.00E-131
55	460	Conjugative transfer protein TrbL	<i>Pseudomonas aeruginosa</i>	FIU24_22485	100	95.88	0.0
56	235	Conjugative transfer protein TrbF	<i>Pseudomonas aeruginosa</i>	MBI8613852.1	100	98.72	3.00E-168
57	333	Conjugative transfer protein TrbG	<i>Pseudomonas aeruginosa</i>	PERCYII40_2686	100	97.85	0.0
58	423	Conjugative transfer protein TrbI	<i>Pseudomonas aeruginosa</i>	WP_023127271.1	100	98.79	0.0
59	82	Hypothetical protein	<i>Proteobacteria</i>	WP_100441186	100	100.00	7.00E-51
60	401	Putative membrane protein	<i>Pseudomonas putida</i>	PP_4492			

ORFs in ICE element integrated in EM2-4. Shaded in different grey tones are the three different sets of genes on the ICE.

estimated for each condition based on their respective spectral counts and normalized spectral abundance and the whole-cell proteomes were compared on the basis of their detection in the three replicates. Data are reported in Table S2. Figure 2 shows a general overview of the functional categories of the whole cell proteome, weighted by the Normalized Spectral Abundance Factor (Zybailov et al., 2006) of the identified proteins in all conditions tested. Proteins involved in central metabolism comprised nearly 67% of total proteins in terms of quantities of the whole cell proteomes. Proteins involved in translation and transcription, cell envelope biogenesis and cell motility and secretion represented each about 10% of total proteins (see Figure 2). These ratios are similar to those reported previously for *Pseudomonas* with other C-sources (Cuenca et al., 2016a). This global view of *P. putida* EM2-4 protein content indicates no specific bias in the proteomic strategy and points to central metabolism as key octane-related functional categories for analysis. Using a log 2-fold change threshold equal or above 1.5 and a stringent statistical level of confidence (q -value <0.05), a list of 89 proteins was identified as statistically significant more abundant in the octane grown than in the glucose grown (Table S3), while 37 proteins were less abundant in the whole-cell proteome in cells growing with octane (Table S4).

Insights into octane metabolism based on proteomic analysis

Octane needs to enter into EM2-4 cells for oxidation and we identified an uncharacterized porin PP_2662 that was 25-fold more abundant in octane grown than

in glucose grown cells and two porins, OprD and OpdD, involved in amino-acid uptake that were induced five-fold. It is likely that octane enters into the periplasmic space through these porins (Table S3, Doncheva et al., 2019). Octane is then oxidized to octanol and subsequently to octanal at the membrane level, and eventually to octanoic acid.

Regarding oxidation of octane by EM2-4, we wish to emphasize that host proteins may support the initial oxidation steps up to octanal and of the latter to octanoic as we found that a PQQ-dependent alcohol dehydrogenase (PP_2679) and an aldehyde dehydrogenase (PP_2680) were induced. This agrees with the notion that octane is being oxidized to octanoic acid.

Among the proteins with the higher fold change were enzymes related to acylation of medium-chain fatty acids, the β -oxidation cycle and the glyoxylate shunt (Table S3 and Figure 3). We identified a set of enzymes involved in the potential acylation of octanoic acid and its subsequent β -oxidation. The corresponding proteins were induced between 10- and 86-fold, with the highest induction found for two acyl-CoA dehydrogenase (PP_4948, PP_0370) (see Table S3) which are involved in each cycle of β -oxidation and yield a *trans*-double bond between C2 and C3, which is the substrate of β -keto-thiolases (PP_2137 and PP_3754) that are also induced (7- to 18.4-fold) (Table S3). In addition, acyl-CoA synthetases PP_2351 and PP_4487 were induced 4.7- and 8.7-fold, respectively. Figure 4 shows a STRING-derived interactome. This figure shows that, among the proteins highly induced in the presence of octane, there were a set of membrane proteins (PP_2662, PP_2663, PP_2667, PP_2669, PP_2674, PP_2675, PP_2678, PP_2679 and PP_2680).

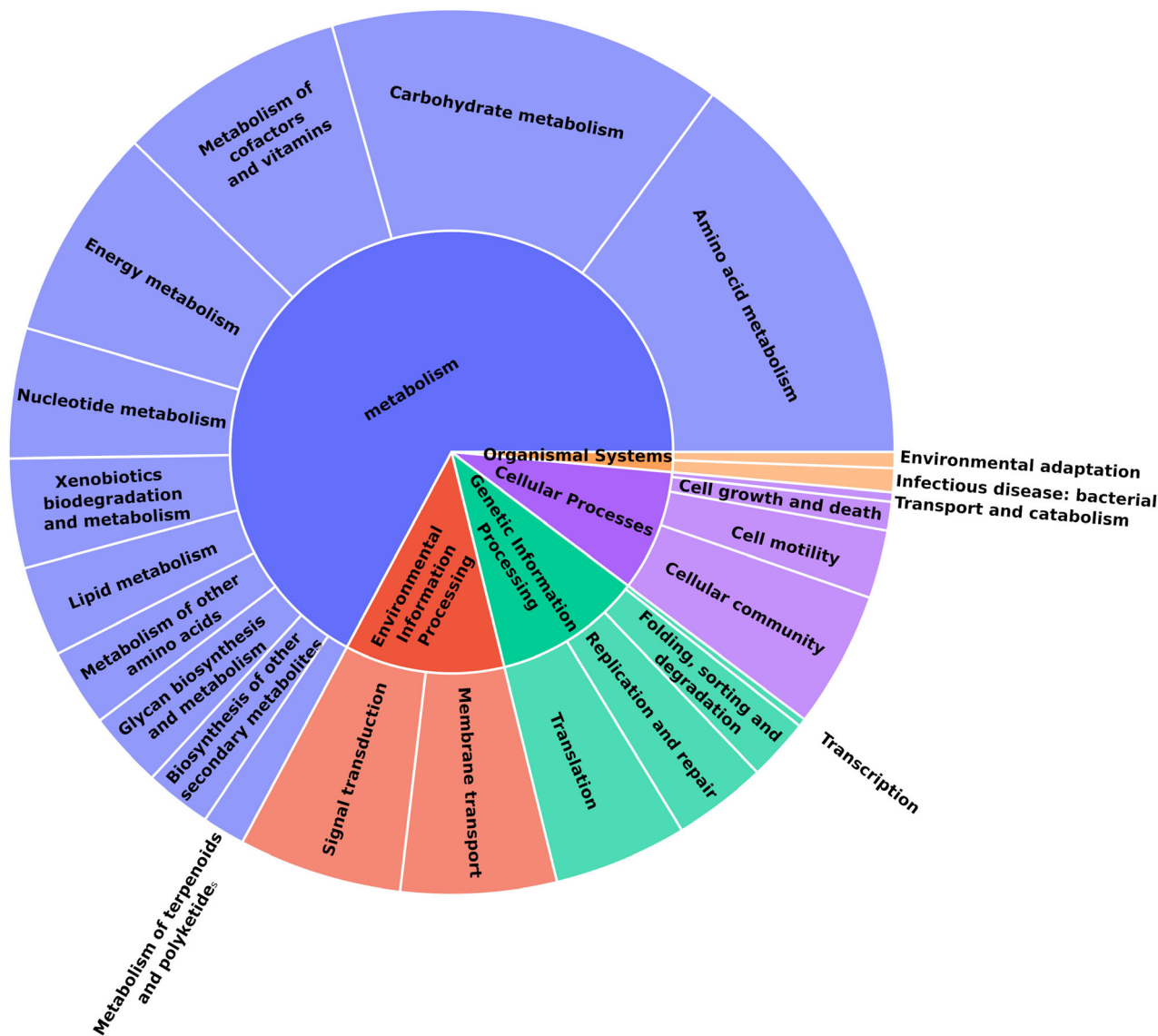


FIGURE 2 Proteomic analysis. Functional categories of proteins displaying loss or gain in cells grown in glucose or octane. Relative quantities of proteins (NSFA) detected in whole-cell proteome. Proteins (67%) belonged to cell metabolism while 10%, 95% and 11% of proteins were related to DNA transcription/translation, cell envelope and functional organelles

The second highest fold change (40-fold) was isocitrate lyase (PP_4116) (Table S3), a protein that is involved in central metabolism through its role in the glyoxylate shunt, where glyoxylate is subsequently converted to malate and, as expected, malate synthase (PP_0356, GcbB) was induced (7.1-fold) (Figure 3, Table S3). Concomitantly, isocitrate dehydrogenase and oxo-glutarate dehydrogenase, two key enzymes of the Krebs cycle were strongly repressed, which supports blockage of the TCA cycle and full operation of the glyoxylate shunt (Table S4). To further confirm the role of the glyoxylate shunt in octane assimilation we generated an *aceA* mutant by homologous recombination using a Km^R cassette that interrupted the *aceA* gene (see Supplementary Experimental procedures). The Km^R *aceA* mutant failed to grow on octane and

butanol as expected. We also found induced 4.5- to 7-fold enzymes that are involved in polyhydroxyalkanoate (PHA) synthesis (PP_5007 and PP_5008), suggesting that excess carbon is stored in the form of PHA. This was confirmed by transmission electron microscopy of cells growing on octane as the sole C source (data not shown).

PP_4203, an electron transfer flavoprotein-ubiquinone oxidoreductase, a cytochrome (PP_2675) and *cbb3-2* terminal cytochrome oxidase (PP_4256, PP_4255, PP_4258 and PP_4257) were also induced. The induction of this set of respiratory proteins is concomitant with repression of another ubiquinol oxidase involved in electron transfer (PP_4651) and several cytochromes (PP_0813, PP_0105, PP_4193, PP_4251 and PP_4250). This suggests that octane utilization

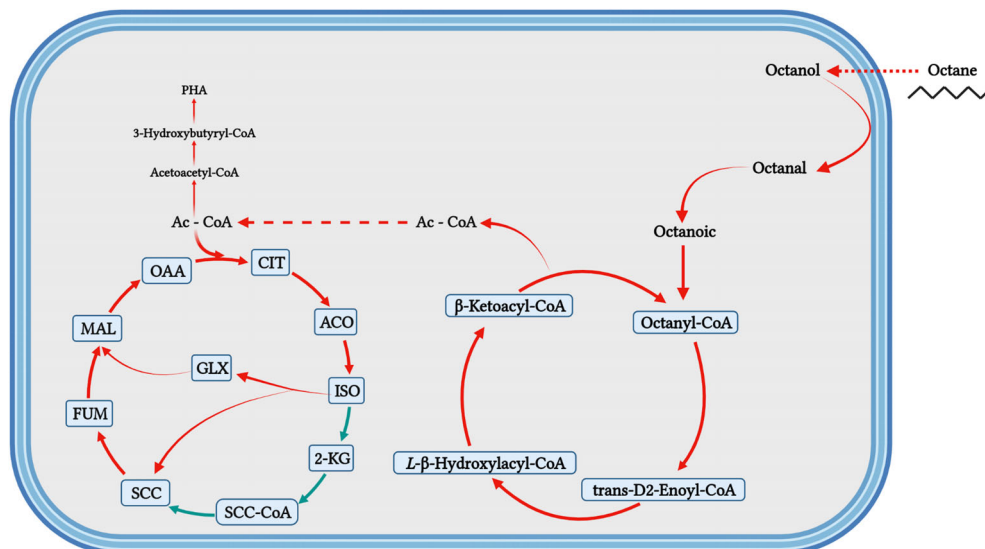


FIGURE 3 Schematic representation of octane metabolism in the EM2-4. Octane likely enters the cells via porins and is oxidized to octanoic acid at the membrane level. Upon acylation it enters the β -oxidation cycle which yields acetyl-CoA that is metabolized via the glyoxylate shunt with excess acetyl-CoA channelled to PHA for storage. Red arrows indicate the cycles under operation with octane and the green arrows indicate the two steps missing in the Krebs cycle in octane-growing cells

leads to optimization of electron flow by synthesis and removal of a series of electron transfer protein from the respiratory chain.

Octane exerts stress in the cells and a number of defence strategies were activated in response to this linear hydrocarbon, for example, the chaperon IbpA was induced 12-fold (Table S3), as well as an efflux pump (PP_2019), and an alkyl-hydro peroxidase induced over fivefold. The histone-like HU protein was also induced fivefold (Table S3) suggesting a potential role in maintenance of internal chromosome structure.

We did not identify an increase in the alkane monooxygenase component or the adjacently encoded alcohol dehydrogenase, which suggests that the *oct* gene cluster may be expressed constitutively. This is in agreement with the absence of specific *alkS/alkT* regulatory genes, although other regulators were found adjacent to these catabolic genes in the island. Pathway evolution is thought to follow this route: for hydrocarbon degradation it has been proposed that cells first acquire the catabolic capacity and later the regulatory genes (Pérez-Pantoja et al., 2021). This may also be the case with the acquired *oct* genes.

In the same vein, we did not see changes in the level of the *cis-trans* isomerase, in spite of the above experimental data showing a *cis* to *trans* isomerization of unsaturated fatty acids (Table S1) (Junker & Ramos, 1999). This agrees with previous observations that *cti* isomerase in several strains of *Pseudomonas* is expressed constitutively (Junker & Ramos, 1999) and became functional once exposed to different toxic compounds. As such, responses to toxic hydrocarbons

through phospholipid modification are an inherent and constitutive function in *Pseudomonas*, regardless of the biodegradative potential of the strain.

Simultaneous degradation of aromatic and lineal hydrocarbons by *P. putida* EM2-4

Toluene, xylenes and their corresponding alcohols [benzyl alcohol/3-methylbenzyl alcohol (3MBA)] and acids [benzoate/3-methylbenzoate (3MBz)] are degraded by enzymes that are encoded by the TOL plasmid (Worsey & Williams, 1975). However, octane is degraded by a hybrid OCT pathway located on the host chromosome. We devised a way to test whether, in EM2-4, octane can be degraded simultaneously with one of three molecules: (i) glucose, which is metabolized through the Entner–Doudoroff pathway, (ii) the TOL upper pathway substrate 3MBA, or (iii) the TOL lower pathway substrate 3MBz. EM2-4 cells were grown on glucose in the absence and in the presence of hydrocarbons and when cells reached a turbidity of about 1 cells were harvested and suspended at a turbidity OD_{660} of 10 to prepare resting cells. Degradation assays were set up with 50 ppm octane and 3 mM glucose, 1 mM 3MBA or 1 mM 3MBz. We then measured the C-source concentrations over time. In accordance with the constitutive expression of the OCT pathway we found that regardless of an additional C-source, octane was removed at a rate of 4.1 ± 0.4 to 15.6 ± 2.0 $\text{mg L}^{-1} \text{h}^{-1}$ (Table 2). In fact, octane degradation rate was highest with glucose—an observation that could be

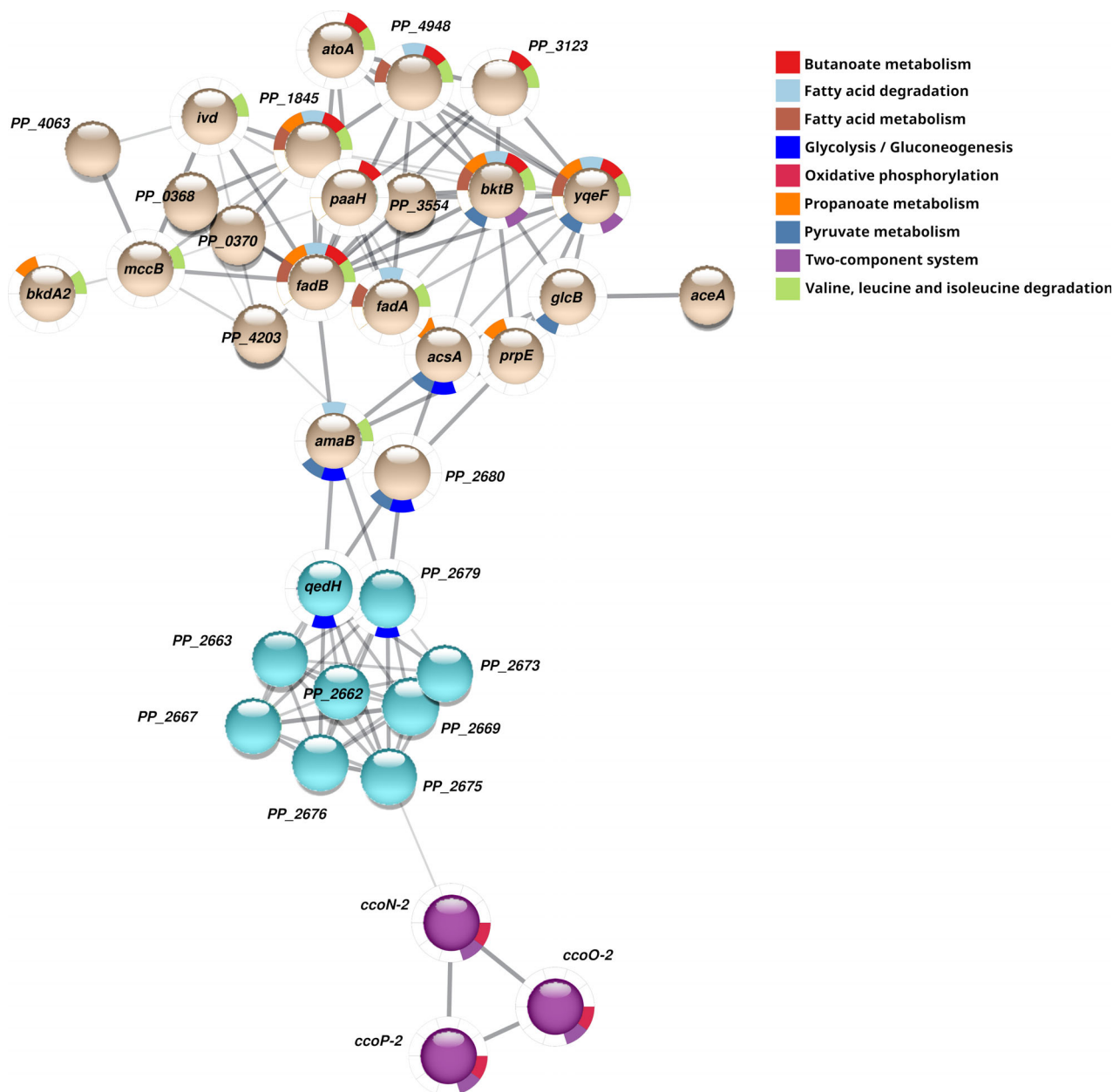


FIGURE 4 STRING-derived interactome of a set of highly abundant proteins in cells growing in octane. The scheme shows that the glyoxylate shunt AceA and GcbB proteins, the set of enzymes related to acylation of medium-chain fatty acids and the β -oxidation cycle

TABLE 2 Rates of OCT and TOL pathways substrate consumption by EM2-4 resting cells.

	Substrate consumption rate at 2 h ($\text{mg L}^{-1} \text{h}^{-1}$)		
	<i>n</i> -octane	Glucose	3MBA or 3MBz
<i>n</i> -octane	4.1	n.a.	n.a.
<i>n</i> -octane + glucose	15.6	544.4	n.a.
<i>n</i> -octane + 3MBA	4.2	n.a.	24.2
<i>n</i> -octane + 3MBz	5.0	n.a.	12.5

The consumption rate is $r = (c \text{ substrate at } t_0 - c \text{ substrate at } t_1) / (t_1 - t_0)$. Octane or aromatic compounds substrate consumption rate (r) was determined for the initial 2 h of the assay, while the glucose consumption rate was determined during the initial 60 min. The displayed values are the mean of at least three independent assays. Standard deviations are between 10% and 20% of the provided values.

explained by the fact that energy generation from glucose could favour cell metabolism. We also found that TOL pathway substrates were consumed at a rate of

12–24 $\text{mg L}^{-1} \text{h}^{-1}$ in the absence and in the presence of octane. Therefore, the EM2-4 strain has the ability to degrade several pollutants simultaneously.

CONCLUSIONS

Pseudomonas putida (pWW0) acquired an ICE with *oct* genes from a microbial community, that allowed oxidation of octane to octanoic acid, the clone was named EM2-4 and it was characterized. The acquired *oct* cluster was atypical in the sense that it lacked the required electron transfer proteins, which were ‘parasitized’ from the host. Once octanoic acid is made, it is acylated and degraded via β -oxidation to produce high levels of acetyl-CoA, which is metabolized through the glyoxylate shunt (Figure 3). In agreement with this proposal, the set of enzymes involved in β -oxidation and the glyoxylate shunt was induced, and a mutant in *aceA* failed to grow on octane or octanoic acid. Our proteomic analysis revealed a redundancy of acyl-CoA and β -oxidation enzymes induced in octane growing cells, which agrees with the fact that no mutants unable to grow on octane in this set of enzymes were found. We have previously generated a collection of mutants in KT2440 and found mutants in several of these enzymes. All of them grew on butanol, supporting the referenced redundancy of acylating enzymes related above. Accordingly, with operation of the glyoxylate shunt, isocitrate lyase—a key enzyme of the pathway—was one of the most abundant proteins when octane was used as the sole C. In a previous study, other mutations in the glyoxylate shunt were found, i.e. in malate synthase (GcbB), that limited the catabolism of butanol. This mutant failed to use octanoic acid (not shown). Therefore, the set of induced proteins and mutants support that medium-chain alkanes are metabolized and β -oxidized to acetyl-CoA, which is channelled to central metabolism via the glyoxylate shunt, while the Krebs cycle playing a minor role. Meanwhile, respiratory chains adapt to optimize electron flow and growth using octane under aerobic conditions.

ACKNOWLEDGEMENTS


Work in Granada was supported by grant KBBE from the European Commission and RTI2018-094370-B-I00 from The Agencia Estatal de Investigación (MINECO) and FEDER Funds, and REC-EU/VAP-CSIC Interdisciplinary Platform (PTI+) for sustainable Plastics towards a circular economy (PTI-SusPlast+). FAME GC–MS analyses were carried out at the Instrumental Technical Services of the Estación Experimental del Zaidín (CSIC), Granada, Spain, by Rafael Nuñez. n-Octane GC–MS analysis was developed by José Miguel Ramos at the Scientific Instrumental Service at the University of Granada, Granada Spain.

ORCID

Estrella Duque  <https://orcid.org/0000-0002-4857-8974>

Zulema Udaondo  <https://orcid.org/0000-0003-3445-6842>

Lázaro Molina  <https://orcid.org/0000-0002-8483-9203>

Juan L. Ramos  <https://orcid.org/0000-0002-8731-7435>

REFERENCES

- Alonso, H. & Roujeinikova, A. (2012) Characterization and two-dimensional crystallization of membrane component ALKB of medium-chain alkane hydroxylase system from *Pseudomonas putida* GoP1. *Applied and Environmental Microbiology*, 78, 7946–7953.
- Altelaar, A.F.M., Frese, C., Preisinger, C., Hennrich, M.L., Schram, A. N., Timmers, M. et al. (2013) Benchmarking stable isotope labeling based quantitative proteomics. *Journal of Proteomics*, 88, 14–26.
- Bagdasarian, M., Lurz, R., Rückert, B., Franklin, F.C., Bagdasarian, M.M., Frey, J. et al. (1981) Specific-purpose plasmid cloning vectors. II. Broad host range, high copy number, RSF1010-derived vectors, and a host-vector system for gene cloning in *Pseudomonas*. *Gene*, 16, 237–247.
- Beites, T. & Mendes, M.V. (2015) Chassis optimization as a cornerstone for the application of synthetic biology based strategies in microbial secondary metabolism. *Frontiers in Microbiology*, 6, 906. <https://doi.org/10.3389/fmicb.2015.00906>
- Belda, E., van Heck, R.G.A., Lopez-Sanchez, M.J., Cruveiller, S., Barbe, V., Fraser, C. et al. (2016) The revisited genome of *Pseudomonas putida* KT2440 enlightens its value as a robust metabolic chassis. *Environmental Microbiology*, 18, 3403–3424.
- Brooks, S.M. & Alper, H.S. (2021) Applications, challenges and needs for employing synthetic biology beyond the lab. *Nature Communications*, 12, 1390.
- Calero, P. & Nikel, P. (2019) Chasing bacterial chassis for metabolic engineering: a perspective review from classical to non-traditional microorganisms. *Microbial Biotechnology*, 12, 98–124.
- Chen, Q., Janssen, D.B. & Witholt, B. (1995) Growth on octane alters membrane lipid fatty acids of *Pseudomonas oleovorans* due to induction of *alkB* and synthesis of octanol. *Journal of Bacteriology*, 177, 6894–6901.
- Cuenca, M.S., Molina-Santiago, C., Gómez-García, M.R. & Ramos, J.L. (2016a) A *Pseudomonas putida* double mutant deficient in butanol assimilation: a promising step for engineering a biological biofuel production platform. *FEMS Microbiology Reviews*, 39, 555–566. <https://doi.org/10.1093/femsre/fuv006>
- Cuenca, M.S., Roca, A., Molina-Santiago, C., Duque, E., Gomez-Garcia, M.R. & Ramos, J.L. (2016b) Understanding butanol tolerance and assimilation in *Pseudomonas putida* BIRD-1: an integrated omics approach. *Microbial Biotechnology*, 9, 100–115.
- Danso, D., Chow, J. & Streit, W.R. (2019) Plastics: environmental and biotechnological perspectives on microbial degradation. *Applied and Environmental Microbiology*, 85, e1095-19.
- Del Castillo, M.T., Duque, E. & Ramos, J.L. (2008) A set of activators and repressors control peripheral glucose pathway in *Pseudomonas putida* to yield common central intermediates. *Journal of Bacteriology*, 190, 2331–2339.
- Doncheva, N.T., Morris, J.H., Gorodkin, J. & Jensen, L.J. (2019) Cytoscape stringApp: network analysis and visualization of proteomics data. *Journal of Proteome Research*, 18, 623–632.
- García-Franco, A., Godoy, P., de la Torre, J., Duque, E. & Ramos, J. L. (2021) United Nations sustainability development goals approached from the side of the biological production of fuels. *Microbial Biotechnology*, 14, 1871–1877. <https://doi.org/10.1111/1751-7915.13912>
- Godoy, P., García-Franco, A., Recio, M.I., Ramos, J.L. & Duque, E. (2021) Synthesis of aromatic amino acids from 2G lignocellulosic substrates. *Microbial Biotechnology*, 14, 1931–1941.

- Herrero, M., de Lorenzo, V. & Timmis, K.N. (1990) Transposon vectors containing non-antibiotic resistance selection markers for cloning and stable chromosomal insertion of foreign genes in Gram-negative bacteria. *Journal of Bacteriology*, 172, 6557–6567.
- Johnson, C.M. & Grossman, A.D. (2015) Integrative and conjugative elements (ICEs): what they do and how they work. *Annual Review of Genetics*, 49, 577–601.
- Junker, F. & Ramos, J.L. (1999) Involvement of the *cis/trans* isomerase Cti in solvent resistance of *Pseudomonas putida* DOT-T1E. *Journal of Bacteriology*, 181, 5693–5700.
- Kampers, L.F.C., Volkers, R.J.M. & Martins dos Santos, V.A.P. (2019) *Pseudomonas putida* KT2440 is HV1 certified, not GRAS. *Microbial Biotechnology*, 12, 845–848.
- Li, X., Xie, Y., Liu, M., Sun, J., Deng, Z. & Ou, H.Y. (2018) oriTfinder: a web-based tool for the identification of origin of transfer in DNA sequences of bacterial mobile genetic elements. *Nucleic Acids Research*, 46(W1), W229–W234.
- Li, Y.P., Pan, J.C. & Ma, Y.L. (2019) Elucidation of multiple alkane hydroxylase systems in biodegradation of crude oil *n*-alkane pollution by *Pseudomonas aeruginosa* DN1. *Journal of Applied Microbiology*, 128, 151–160.
- Liu, M., Li, X., Xie, Y., Bi, D., Sun, J., Li, J. et al. (2019) ICEberg 2.0 an updated database of bacterial integrative and conjugative elements. *Nucleic Acids Research*, 47, D660–D665. <https://doi.org/10.1093/nar/gky1123>
- Liu, J.M., Solem, C. & Jensen, P.R. (2020) Harnessing biocompatible chemistry for developing improved and novel microbial cell factories. *Microbial Biotechnology*, 13, 54–66.
- Matilla, M.A., Espinosa-Urgel, M., Rodríguez-Herva, J.J., Ramos, J.L. & Ramos-González, M.I. (2007) Genomic analysis reveals the major driving forces of bacterial life in the rhizosphere. *Genome Biology*, 8, R179.
- Molina, L., Ramos, C., Duque, E., Ronchel, C., García, J.M., Wyke, L. et al. (2000) Survival of *Pseudomonas putida* KT2440 in soil and in the rhizosphere of plants under greenhouse and environmental conditions. *Soil Biology and Biochemistry*, 32, 315–321.
- Molina, L., La Rossa, R., Nogales, J. & Rojo, F. (2019) *Pseudomonas putida* KT2440 metabolism undergoes sequential modifications during exponential growth phase in a complete medium as compounds gradually consumed. *Environmental Microbiology*, 21, 2375–2390.
- Molina-Santiago, C., Daddaoua, A., Fillet, S., Duque, E. & Ramos, J.L. (2014) Interspecies signaling: *Pseudomonas putida* efflux pump TtgGHI is activated by indole to increase antibiotic resistance. *Environmental Microbiology*, 16, 1267–1281.
- Mori, J.F. & Kanaly, R.A. (2021) Multispecies diesel fuel biodegradation and niche formation are initiated by pioneer hydrocarbon-utilizing proteobacteria in a soil bacterial consortium. *Applied and Environmental Microbiology*, 87, e02268-20. <https://doi.org/10.1128/AEM.02268-20>
- Nagata, Y., Kato, H., Ohtsubo, Y. & Tsuda, M. (2019) Lesson from the genomes of lindane-degrading sphingomonads. *Environmental Microbiology Reports*, 11, 630–644.
- Nakazawa, T. (2002) Travels of a *Pseudomonas*, from Japan around the world. *Environmental Microbiology*, 4, 782–786.
- Nelson, K.E., Weinel, C., Paulsen, I.T., Dodson, R.J., Hilbert, H., Martins dos Santos, V.A.P. et al. (2002) Complete genome sequence and comparative analysis of the metabolically versatile *Pseudomonas putida* KT2440. *Environmental Microbiology*, 4, 799–808.
- Nikel, P.I. & de Lorenzo, V. (2013) Engineering an anaerobic metabolic regime in *Pseudomonas putida* KT2440 for the anoxic biodegradation of 1,3-dichloroprop-1-ene. *Metabolic Engineering*, 15, 98–112.
- Nikel, I. & de Lorenzo, V. (2014) Robustness of *Pseudomonas putida* KT2440 as a host for ethanol biosynthesis. *New Biotechnology*, 31(6), 562–571.
- Nikel, P.I. & de Lorenzo, V. (2018) *Pseudomonas putida* as a functional chassis for industrial biocatalysis: from native biochemistry to *trans*-metabolism. *Metabolic Engineering*, 50, 142–155.
- Niqui-Arroyo, J. L., Fernández-Cifuentes, S., Roca-Hernández, A. & Solano-Parada, J. (2013) *Procedimiento biológico para la degradación de mezclas complejas de hidrocarburos en fase acuosa*. Patent ES2491965.
- Nogales, J., Mueller, J., Gudmundson, S., Canalejo, F.J., Duque, E., Ramos, J.L. et al. (2020) High-quality genome-scale metabolic modelling of *Pseudomonas putida* highlights its broad metabolic capabilities. *Environmental Microbiology*, 22, 255–269.
- Pérez-Pantoja, D., Nikel, P.I., Chavarria, M. & de Lorenzo, V. (2021) Transcriptional control of 2,4-dinitrotoluene degradation in *Burkholderia* sp. R34 bears a regulatory patch that eases pathway evolution. *Environmental Microbiology*, 23, 2522–2531.
- Pizarro-Tobias, P., Niqui, J.L., Roca, A., Solano, J., Fernández, M., Bastida, F. et al. (2015) Field-trial on removal of petroleum-hydrocarbon pollutants using a microbial consortium for bioremediation and rhizoremediation. *Environmental Microbiology Reports*, 7, 83–94.
- Poblete-Castro, I., Binger, D., Rodrigues, A., Becker, J., Martins dos Santos, V.A.P. & Wittmann, C. (2013) In-silico-driven metabolic engineering of *Pseudomonas putida* for enhanced production of poly-hydroxyalkanoates. *Metabolic Engineering*, 15, 113–123.
- Poblete-Castro, I., Wittmann, C. & Nikel, P.I. (2020) Biochemistry, genetics and biotechnology of glycerol utilization in *Pseudomonas* species. *Microbial Biotechnology*, 13, 32–53.
- Ramos, J.L. & Duque, E. (2019) Twenty-first century chemical odyssey: fuels versus commodities and cell factories versus chemical plants. *Microbial Biotechnology*, 12, 200–209. <https://doi.org/10.1111/1751-7915.13379>
- Ramos, J.L. & Timmis, K.N. (1987) Experimental evolution of catabolic pathways of bacteria. *Microbiological Sciences*, 4, 228–237.
- Ramos, J.L., Wasserfallen, A., Rose, K. & Timmis, K.N. (1987) Redesigning metabolic routes: manipulation of TOL plasmid pathway for catabolism of alkylbenzoates. *Science*, 235, 593–596.
- Ramos, J.L., Cuenca, M.S., Molina-Santiago, C., Segura, A., Duque, E., Gómez-García, M.R. et al. (2015) Mechanisms of solvent resistance mediated by interplay of cellular factors in *Pseudomonas putida*. *FEMS Microbiology Reviews*, 39, 555–566.
- Reed, K.B. & Alper, H.S. (2018) Expanding beyond canonical metabolism: Interfacing alternative elements, synthetic biology, and metabolic engineering. *Synthetic and Systems Biotechnology*, 3, 20–33.
- Reineke, W. & Knackmuss, H.J. (1988) Microbial degradation of haloaromatics. *Annual Review of Microbiology*, 42, 263–287.
- Rojo, F. (2009) Degradation of alkanes by bacteria. *Environmental Microbiology*, 11, 2477–2490.
- Ronchel, M.C. & Ramos, J.L. (2001) Dual system to reinforce biological containment of recombinant bacteria designed for rhizoremediation. *Applied and Environmental Microbiology*, 67, 2649–2656.
- Timmis, K.N. (2002) *Pseudomonas putida*: a cosmopolitan opportunist par excellence. *Environmental Microbiology*, 4, 779–781.
- Udaondo, Z., Duque, E., Fernández, M., Molina, L., de la Torre, J., Bernal, P. et al. (2012) Analysis of solvent tolerance in *Pseudomonas putida* DOT-T1E based on its genome sequence and a collection of mutants. *FEBS Letters*, 586(18), 2932–2938.
- Udaondo, Z., Molina, L., Segura, A., Duque, E. & Ramos, J.L. (2016) Analysis of the core genome and pangenome of *Pseudomonas putida*. *Environmental Microbiology*, 118, 3268–3283.
- Whyte, L.G., Bourbonnière, L. & Greer, C.N. (1997) Biodegradation of petroleum hydrocarbons by psychotrophic *Pseudomonas* strains possessing both alkane (*alk*) and naphthalene (*nah*) catabolic pathways. *Applied and Environmental Microbiology*, 63, 3719–3723.
- Worsey, M.J. & Williams, P.J. (1975) Metabolism of toluene and xylenes by *Pseudomonas putida* (arvilla) mt-2: evidence for new function of the TOL plasmid. *Journal of Bacteriology*, 124, 7–13.

- Zybilov, B., Mosley, A.L., Sardi, M.E., Coleman, M.K. & Washburn, M.P. (2006) Statistical analysis of membrane proteome expression changes in *Saccharomyces cerevisiae*. *Journal of Proteome Research*, 5, 2339–2347.
- Zylstra, G.J. & Gibson, D.T. (1989) Toluene degradation by *Pseudomonas putida* F1: nucleotide sequence of the *tod C1C2BADE* genes and their expression in *Escherichia coli*. *The Journal of Biological Chemistry*, 264, 14940–14946.

SUPPORTING INFORMATION

Additional supporting information may be found in the online version of the article at the publisher's website.

How to cite this article: Duque, E., Udaondo, Z., Molina, L., de la Torre, J., Godoy, P. & Ramos, J. L. (2022) Providing octane degradation capability to *Pseudomonas putida* KT2440 through the horizontal acquisition of *oct* genes located on an integrative and conjugative element. *Environmental Microbiology Reports*, 14(6), 934–946. Available from: <https://doi.org/10.1111/1758-2229.13097>